Ion Binding Affinity in the Cavity of the KcsA Potassium Channel†

Yufeng Zhou‡ and Roderick MacKinnon*

Howard Hughes Medical Institute and Laboratory of Molecular Neurobiology and Biophysics, Rockefeller University, 1230 York Avenue, New York, New York 10021

Received January 15, 2004; Revised Manuscript Received March 1, 2004

ABSTRACT: The hydrophobic cell membrane interior presents a large energy barrier for ions to permeate. Potassium channels reduce this barrier by creating a water-filled cavity at the middle of their ion conduction pore to allow ion hydration and by directing the C-terminal "end charge" of four α-helices toward the water-filled cavity. Here we have studied the interaction of monovalent cations with the cavity of the KcsA K^+ channel using X-ray crystallography. In these studies, Tl^+ was used as an analogue for K^+ and the total ion-stabilization energy for Tl^+ in the cavity was estimated by measuring its binding affinity. Binding affinity for the Na^+ ion was also measured, revealing a weak selectivity (∼7-fold) favoring Tl^+ over Na^+. The structures of the cavity containing Na^+, K^+, Tl^+, Rb^+, and Cs^+ are compared. These results are consistent with a fairly large (more negative than −100 mV) electrostatic potential inside the cavity, and they also imply the presence of a weak nonelectrostatic component to a cation's interaction with the cavity.

To move into and out of cells, inorganic ions must overcome a large energy barrier known as the dielectric barrier imposed by the hydrophobic cell membrane interior (*1*). Ions surmount this barrier by diffusing through ion channels, which are cell membrane-spanning proteins specifically designed to lower the dielectric barrier. A prototype of selective ion channels was provided by the structure of the KcsA K^+ channel (*2*, *3*). This channel contains halfway across its ion conduction pore, approximately at the level of the membrane center, a large water-filled cavity containing a K^+ ion (Figure 1). It also has four α-helices, referred to as pore helices, which point their carboxyl termini toward the ion suspended in the center of the water-filled cavity. The ion looks as if to be stabilized by the partial negative charges of the pore helices' C-terminal end.

On the basis of these observations, it has been proposed that K^+ channels overcome the dielectric barrier by surrounding a K^+ ion with water molecules at the center of the membrane, and by stabilizing the ion through electrostatic interactions with oriented pore helices (*2*). A subsequent theoretical analysis lent support to the idea that the cavity and the pore helices are sufficient to overcome the dielectric barrier (*4*). The analysis also suggested that in the cavity monovalent cations are energetically favored over divalent cations due to a balance between attractive (between the ion and the pore helices) and repulsive (between the ion and the membrane) electrostatic forces that are optimized for monovalent cations (*4*).

The discovery of the cavity provided a general explanation for how a K^+ channel overcomes the dielectric barrier, while at the same time it raised many specific questions regarding the magnitude of different energy terms. For example, with what affinity does a K^+ ion "bind" in the cavity, and are the interactions between this ion and the channel exclusively electrostatic? In the present study, we begin to address these questions through an analysis of crystal structures of KcsA determined in various ionic conditions.

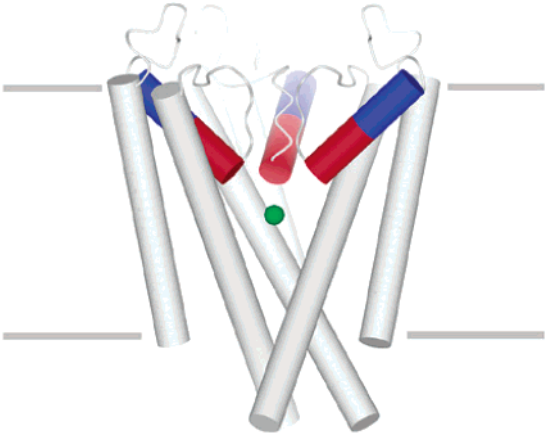

FIGURE 1: The structure of the KcsA potassium channel. Three subunits of the tetrameric channel are shown in cylinder and coil representation. The pore helices point their partial negative charge (red represents the C-termini and blue represents the N-termini) toward the center of the cavity where an ion (green sphere) is located. The gray lines indicate the boundary of the membrane bilayer. Figures 1, 2a, and 4 were prepared with Bobscript (*17*) and Raster3D (*18*).

METHODS

To obtain high-quality diffraction data, we cocrystallized KcsA with an antibody Fab fragment. The purification and crystallization procedures were similar to those described previously (*3*), except before crystallization an additional dialysis step was carried out to exchange the complex into

† This work was supported by NIH Grant GM47400. R.M. is an investigator in the Howard Hughes Medical Institute.

* To whom correspondence should be addressed. E-mail: mackinn@rockefeller.edu. Phone: (212) 327−7288. Fax: (212) 327−7289.

‡ Current Address: Department of Cellular and Molecular Physiology, Yale University School of Medicine, 333 Cedar Street, New Haven, CT 06520.

10.1021/bi049876z CCC: $27.50
Published on Web 04/08/2004

Table 1: Crystallographic Data and Refinement Statistics

salt concentration					refinement statistics
$TlNO_3$ (mM)	$NaNO_3$ (mM)	resolution (Å)	R_{sym}[a]	completeness (%)	R_{free}/R_{work} (%)[b]
3	237	2.9	0.095	92.9	24.3/21.2
25	215	2.8	0.136	99.8	27.3/23.8
65	175	2.3	0.083	100	29.2/27.1
80	160	2.9	0.103	96.6	30.6/26.1
100	140	2.4	0.093	99.8	24.9/21.8
160	80	1.9	0.069	97.1	22.8/20.8
240	0	2.8	0.107	96.3	28.1/23.1
170	0	2.6	0.099	98.5	34.5/29.1
100	0	2.6	0.102	97.7	32.0/27.9
50	0	3.0	0.109	100	31.8/26.9

[a] $R_{sym} = \sum|I_i - \langle I_i\rangle|/\sum I_i$, where $\langle I_i\rangle$ is the average intensity of symmetry-equivalent reflections. [b] $R = \sum|F_o - F_c|/\sum F_o$, 5 or 10% of the data that were excluded in refinement were used in the R_{free} calculation.

desired ionic conditions. For growing crystals in Tl^+, the dialysis buffers contained 50 mM Hepes (pH 7.5), 5 mM decyl-maltoside (DM),[1] and different concentrations of either $TlNO_3$ or mixtures of $TlNO_3$ and $NaNO_3$ (Table 1). For growing crystals in Rb^+ and Cs^+, the dialysis buffers contained 50 mM Tris (pH 7.5), 5 mM DM, and 150 mM RbCl or CsCl, as described (*5*). All the crystals used in this study diffract X-rays to Bragg spacings ranging from 3.0 to 1.9 Å at the Cornell High Energy Synchrotron Source A1 station and the National Synchrotron Light Source X-25 (Table 1). Data were processed with Denzo and Scalepack (*6*). Phases were obtained by molecular replacement using the published KcsA-Fab complex structure (PDB entry 1K4C). Structure refinement was carried out using CNS (*7*) with cycles of model rebuilding using O (*8*). The Fab fragment improves the crystal quality, but it does not change the structure of KcsA (*3*). The RMSD between the structures obtained with and without the Fab fragment (PDB entries 1K4C and 1BL8) is 1.7 Å. For simplicity, the structure of the complex will be referred to only as the KcsA structure in the following discussions. One-dimensional electron density maps were calculated in the cavity as described previously for ions in the selectivity filter (*5*, *9*). Briefly, all the structural models (without ions, waters and lipids) were refined against their corresponding data set (Table 1). All data sets were scaled to 3.0 Å using the 160 mM $T1^+$ data set as the reference set. Difference Fourier maps were calculated using the CCP4 suit (*10*), and one-dimension electron density profiles were obtained by sampling the difference maps along the central axis of the channel using MAPMAN (*11*). The area of the peaks in the profiles were integrated and normalized. Our estimates of cavity ion occupancy in this study are approximate, not absolute. See results for a description of underlying assumptions.

The PDB entries for the KcsA structures solved in high concentration of K^+, Tl^+, Rb^+, and Cs^+ are 1K4C, 1R3J, 1R3I, and 1R3L, respectively. The PDB entries for the structures solved in high concentrations of Na^+ in the presence of low K^+ or Tl^+ are 1K4D and 1R3K, respectively.

RESULTS

Estimating Ion Affinity in the Cavity. We first wish to estimate the affinity of K^+ for the cavity by measuring the relative occupancy of K^+ as a function of K^+ concentration in solution bathing the crystals. To do this, we must determine structures in different K^+ concentrations and quantify the change in electron density at the cavity center: this density should be proportional to the fraction of channels in the crystal that contain a K^+ ion at this position. At the resolution of data in this study, we are not able to separate occupancy from the Debye−Waller (temperature) factor and therefore cannot determine the absolute occupancy of the ion in the cavity at any given K^+ concentration. To estimate ion occupancy, we make two assumptions: first, that when we change ion concentration we affect the ion's occupancy and not its Debye−Waller factor, and second, that a leveling-off of electron density as ion concentration is raised indicates that we are approaching an occupancy of unity.

To improve the signal-to-noise ratio of our measurements, we have used Tl^+ instead of K^+. Tl^+ is a very good analogue of K^+ because its radius (1.40 Å) and dehydration energy (77.6 kcal/mol) are close to that of K^+ (radius 1.33 Å, dehydration energy 76.4 kcal/mol). Like K^+, Tl^+ conducts through K^+ channels, it binds at positions in the selectivity filter identical to K^+, and it does not alter the channel structure to a discernible extent (RMSD between the K^+ and Tl^+ complexes is 0.43 Å) (*5*). For these reasons, we assume that Tl^+ interacts with the cavity in a manner very similar to K^+. The crystallographic advantage to using Tl^+ is an 80-electron signal compared to 18 electrons for K^+. The stronger diffraction signal allows a more accurate measurement of the ion's presence.

In our first experiments, we varied the $TlNO_3$ concentration (which we refer to as Tl^+) in the crystallization solutions while allowing ionic strength to vary. Useful crystals grew only at Tl^+ concentrations of 50 mM and higher; structures were determined for 50, 100, 170, and 240 mM Tl^+. For each concentration, an isomorphous difference Fourier ($F_o - F_c$) map was calculated using a model refined against the data without a cavity ion (an omit map). An example of such a map is shown in Figure 2a. To simplify data presentation and electron density integration, we sampled each of the three-dimensional maps along the central axis of the channel as shown (Figure 2a, dashed line) and plotted one-dimensional electron density maps for each concentration (Figure 2b). In a one-dimensional map, the peak area should be approximately proportional to the number of electrons contributing to the electron density, assuming a constant temperature factor (*5*). We integrated the peaks and divided each area by that measured at 240 mM Tl^+ (the highest concentration).

A graph of the relative areas shows that the electron density in the cavity is nearly constant at concentrations above 100 mM Tl^+, which we interpret to mean that full occupancy is being approached (Figure 2c). In fact, only the 50 mM data point deviates much below unity. By fitting the data to a Langmuir isotherm, we estimate the dissociation constant (K_d) to be approximately 16 mM. This is a very rough estimate because of the absence of data below 50 mM Tl^+ (concentrations at which crystals failed to grow). Because the three highest concentration points are very close to saturation we conclude that the affinity is quite high; if

[1] Abbreviations: DM, *N*-decyl β-D-maltoside; CNS, crystallography and NMR system.

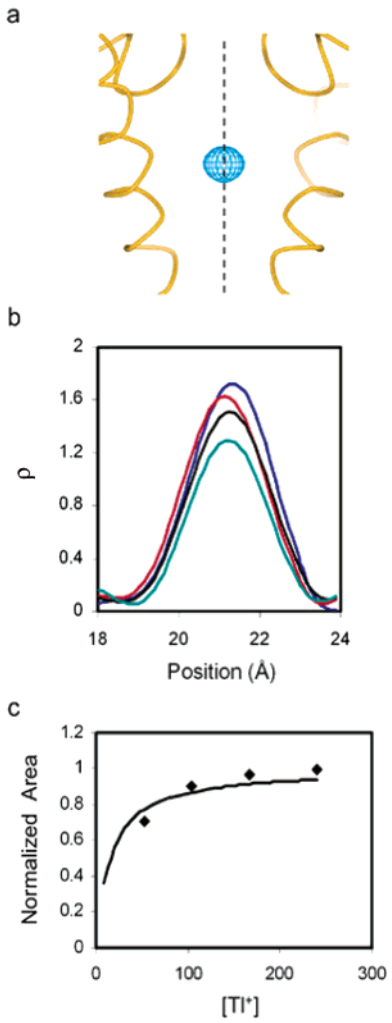

FIGURE 2: The affinity of the KcsA cavity for Tl^+ ion. (a) The blue mesh represents a contoured (3σ) isomorphous difference Fourier ($F_o - F_c$) map calculated using a model refined against the data without a cavity ion. The yellow trace represents the C_α trace of two subunits of KcsA. The dashed line shows the central axis of the channel. (b) Absolute value of electron density (ρ) sampled along the central axis of the channel in an electron density map calculated using the FFT function of CCP4 (*10*) as described in methods. Colors correspond to different concentrations of Tl^+: cyan: 50 mM, black: 100 mM, red: 170 mM and blue: 240 mM. Zero on the *x*-axis corresponds to the level of the C_α of residue 79. (c) The normalized area of peaks in (b) as a function of Tl^+ concentration.

anything, 16 mM (corresponding to a standard state Gibbs Free Energy of −2.5 kcal/mol) is likely to be an over estimate of the K_d (i.e., the true binding affinity is probably greater).

Estimation of Electrostatic Potential in the Cavity. The electrostatic free energy difference between Tl^+ in bulk water versus Tl^+ inside the cavity takes the form:

$$\Delta G(Q) = 0.5AQ^2 + BQ + C \approx 0.5AQ^2 + BQ \quad (1)$$

with Q being the ion charge, A is a polarization constant related to the ion's interaction with its dielectric environment, B is the electrostatic potential due to fixed charges in the ion's environment, and C is a negligibly small (and thus excluded) term (*4*). In eq 1, A and B account for the electrical field interactions (with induced and fixed charges, respectively) of the ion upon transfer from bulk water to the cavity: A is repulsive (positive) due to the low dielectric

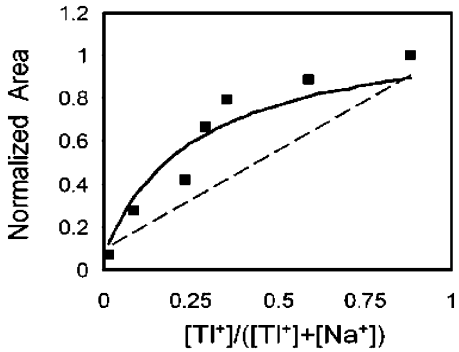

FIGURE 3: The affinity of the KcsA cavity for Na^+ ion. The normalized area of peaks in the electron density profiles is plotted as a function of Tl^+ mole fraction. The total concentration of Tl^+ and Na^+ were kept at 240 mM. The dashed line shows the expected outcome if Tl^+ and Na^+ have the same affinity in the cavity. The solid curve corresponds to eqs 3 and 4 with $K_{d\ Na} = 110$ mM.

membrane compared to bulk water, and B is attractive (negative) due to charges within the protein. If A in eq 1 were zero then the estimated K_d of 16 mM would correspond to approximately −100 mV. Because of the membrane-embedded location of the cavity A is certainly not zero, but is expected to have some positive value (repulsive). Consequently, the fixed potential in the cavity would have to be more negative than −100 mV. Continuum electrostatic calculations suggest that this fixed potential is due largely to the pore helices (*4*).

Na^+ Affinity: Evidence for a Non-Electrostatic Energy Term. We next asked whether Na^+ binds in the cavity with the same affinity as Tl^+. Sodium, because of its smaller radius (0.95 Å), does not easily enter the selectivity filter of a K^+ channel but it can enter the cavity. We are interested in Na^+ because it allows us to ask whether the entire interaction of an ion with the cavity is electrostatic, or is there a nonelectrostatic component? Sodium helps us for the following reason. In the continuum electrostatic theory, to a first approximation the only difference between Na^+ and Tl^+ is the ionic radius. This theory tells us that the energy for transfer of an ion of charge Q and radius r_i from an infinite surrounding of dielectric constant ϵ_1 into a spherical cavity of radius r_c ($r_c > r_i$) filled with a medium of dielectric constant ϵ_1 and surrounded by ϵ_2 is given by eq 2:

$$\Delta G = (0.5/r_c)((\epsilon_1 - \epsilon_2)/(\epsilon_1\epsilon_2))Q^2 \quad (2)$$

Equation 2 corresponds to the "A term" of eq 1 for the simple system of a spherical "water-filled" cavity: in the absence of fixed charges $B = 0$. The interesting point is that the ion transfer energy is independent of ion size. The same should be true for the more complex geometry of the K^+ channel cavity. Thus, any difference in the affinity of Na^+ or K^+ is not explained by a simple continuum electrostatic theory.

We grew crystals of the KcsA−Fab complex in various mixtures of Tl^+ and Na^+, maintaining the ionic strength at 240 mM, and analyzed electron density peaks as described above. The normalized areas for the electron density peaks are graphed as a function of the Tl^+ mole fraction (Figure 3). Since Tl^+ and Na^+ compete for the same binding site, and since 240 mM should be well above the K_d for either ion, we expect there to be either a Tl^+ or a Na^+ ion in the

cavity at any given time. If these two ions have identical affinities, then the total electron density inside the cavity should be directly proportional to (i.e., a linear function of) the Tl^+ mole fraction, with a nonzero *y*-intercept to account for 10 electrons in Na^+ (Figure 3, dashed line). In fact, the data points clearly deviate from a straight line, indicating that the affinities of Na^+ and Tl^+ are not identical.

Before further analysis, we must consider the following issue: at very low concentrations of Tl^+ the selectivity filter, which is adjacent to the cavity (on the extracellular side of the pore), undergoes a change in its conformation (*5*). The very same change also occurs in low concentrations of K^+ (*3*). However, we think that this change has little influence on ion binding in the cavity for the following reasons: first, the orientation of the pore helices and structure of the cavity remains the same in both conformations of the selectivity filter (*3*), and second, the data points in Figure 3a corresponding to channels with low-Tl^+ (first three points) and high-Tl^+ (remainder of points) selectivity filter conformations follow the same trend.

To quantify the relative affinities of Tl^+ and Na^+ we consider the following competitive reaction scheme:

$$\begin{array}{c} \mathrm{KcsA} + \mathrm{Tl}^+ \leftrightarrow \mathrm{KcsA{\bullet}Tl}^+ \\ + \\ \mathrm{Na}^+ \\ \updownarrow \\ \mathrm{KcsA{\bullet}Na}^+ \end{array}$$

The fraction of channels containing Tl^+ in the cavity (θ_{Tl}) is

$$\theta_{Tl} = \frac{1}{\left(1 + \frac{K_{dTl}}{[Tl^+]} + \frac{K_{dTl}[Na^+]}{K_{dNa}[Tl^+]}\right)} \qquad (3)$$

An analogous equation can be written for the fraction of channels containing Na^+ in the cavity (θ_{Na}). The normalized area of the electron density peaks should thus be related to θ_{Tl}, θ_{Na}, and the number of electrons in Tl^+ (80e) and Na^+ (10e) according to

$$\text{area} = (\theta_{Tl}\cdot 80 + \theta_{Na}\cdot 10)/80 \qquad (4)$$

If we apply the result of our first experiment in this study, $K_{d\ Tl} = 16$ mM, to the above equations, the only unknown value is $K_{d\ Na}$. The best fit of eqs 3 and 4 to the data yields $K_{d\ Na} \cong 110$ mM. Thus, the cavity has about a 7-fold preference for Tl^+ over Na^+, corresponding to approximately 1.2 kcal/mol energy difference favoring Tl^+. The accuracy of this result depends on the accuracy of $K_{d\ Tl}$: the lower $K_{d\ Tl}$ is, the lower $K_{d\ Na}$ will be. Regardless of the precise value of the dissociation constant, it is clear that the cavity binds Tl^+ with somewhat higher affinity than Na^+. On the basis of the argument given above, this difference cannot be accounted for by the continuum electrostatic theory. The general form of eq 1 requires another energy term to account for the affinity difference between Tl^+ and Na^+. We do not know the mechanistic origin of this term. As a point of discussion, it is worthwhile to inspect the "structure" of the ion−water complex inside the cavity for monovalent cations of various sizes (Figure 4).

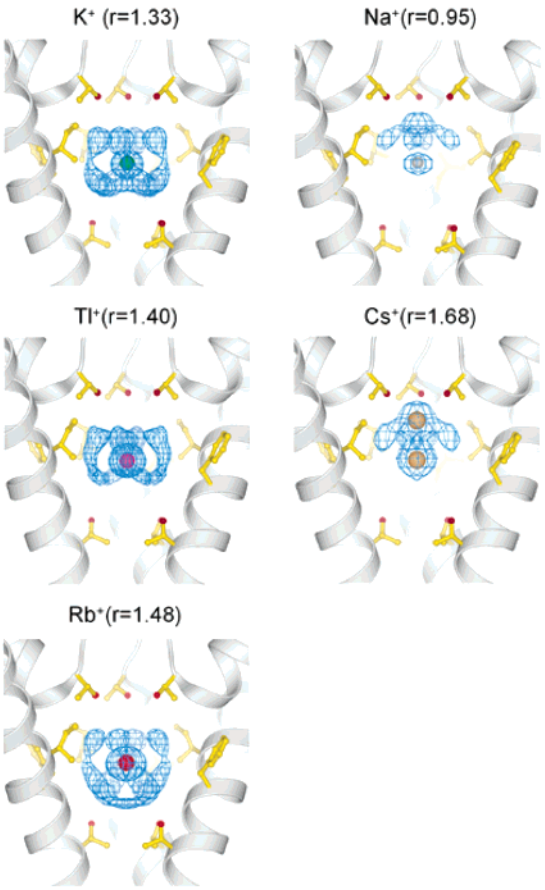

FIGURE 4: Electron densities of different monovalent cations and their hydration shells inside the cavity of the KcsA channel. The C_α trace of KcsA is represented as a gray ribbon. The amino acids forming the lining of the cavity are shown as ball-and-stick. The $F_o - F_c$ omit maps (blue) are countered at 3σ. Ions in the cavity are represented as colored spheres. (PDB entries: 1K4C, 1R3J, 1R3I, 1K4D, and 1R3L).

DISCUSSION

From these experiments, we reach three conclusions. First, Tl^+ binds in the cavity with fairly high affinity ($K_{d\ Tl} \sim 16$ mM). Since K^+ is very similar to Tl^+ in radius, dehydration energy, and binding to the selectivity filter, we expect that it should bind in the cavity with an affinity similar to Tl^+. If this is the case, then under physiological ion concentrations the cavity will be occupied by a K^+ ion nearly all the time. Effectively, the local concentration of K^+ in the cavity, that is, at the intracellular entryway to the selectivity filter, is about 2 M. Second, much of the interaction between the cavity ion and the channel is probably electrostatic because the ion is not in van der Waals contact with any protein atoms. Third, some fraction of the interaction is apparently not electrostatic in origin because we detect an affinity difference between Tl^+ and Na^+, monovalent cations of different radius.

An analysis of Na^+ inhibition of KcsA K^+ channels using electrophysiological methods allowed Miller and Nimigean to determine the selectivity ratio of K^+ and Na^+ for an ion binding site located on the intracellular side of the selectivity filter (*12*). They assumed this site to be in the cavity and

found a 5−7-fold preference for K^+ over Na^+, the same as the selectivity ratio observed in the structural data presented here. In a much earlier study carried out long before the structure of a K^+ channel was known, Neyton and Miller analyzed the effect of internally applied ions on the rate of Ba^{2+} ion dissociation from BK K^+ channels (*13*). They described an ion binding site on the internal side of the channel, which they called the "internal lock-in site", that binds K^+ with a roughly 7 mM K_d and has a 5-fold preference for K^+ over Na^+. Through structural studies Ba^{2+} is now known to block K^+ channels at position 4 in the selectivity filter, immediately adjacent to the cavity (*14*), suggesting that the "internal lock-in site" in BK channels is the cavity. Therefore, in two different K^+ channels, KcsA and BK, electrophysiological studies define a functional site that corresponds extremely well in terms of affinity and selectivity to the cavity ion studied here. The good correspondence between the structural and functional data implies an important property of ion binding in the cavity. The BK and KcsA K^+ channels were open in the electrophysiological studies while KcsA is in a closed conformation in the structural studies. The consistency of results implies therefore that equilibrium ion binding properties of the cavity do not change very much when a K^+ channel undergoes a conformational change from closed to open. A crystal structure of an open K^+ channel called MthK has been determined and the cavity at the level where an ion resides is very similar to that in the closed KcsA K^+ channel (*15*, *16*).

In the absence of additional information, we cannot separate the *A* and *B* energy terms in eq 1. The situation is even more complicated because we have also to account for a third, nonelectrostatic term. For purposes of a thought experiment, however, suppose the nonelectrostatic term is 1.2 kcal/mol for Na^+ and 0 for Tl^+: that is to say, there is something about the cavity that destabilizes Na^+ relative to Tl^+, which itself interacts with the cavity according to eq 1. Next, we can make use of the observation that divalent cations do not appear to enter into the cavity of KcsA (or other K^+ channels that are not of the inward-rectifier class) by applying the inequality $\Delta G(Q = 1) < \Delta G(Q = 2)$. If the affinity of divalent cations is less than that of monovalent cations for electrostatic reasons then the inequality applied to eq 1 requires $A > 2B/3$, or a negative potential in the cavity of 156 mV or greater. Of course, these calculations are highly speculative because there are too many unknowns, but they make the point that the electrostatic potential inside the cavity is likely to be negative and of large magnitude.

Probably the most interesting result in this study, and of previous electrophysiological studies (*12*, *13*) is the aspect we do not understand: selectivity of the cavity for K^+ over Na^+. The selectivity is very weak (~5-fold) compared to what is observed inside the selectivity filter (~10^3−10^4-fold), but it is interesting because its origin is not at all obvious. Figure 4 shows the electron density inside the cavity of structures solved in the presence of high Na^+, K^+, Tl^+, Rb^+, and Cs^+. These monovalent cations range in radius from 0.95 Å (Na^+) to 1.69 Å (Cs^+). Only Cs^+ is obviously anomalous in that it tends to reside at two locations (but not both at once) rather than at a single "energy minimum". Sodium does not have a complete visible hydration shell, but that may be due to a symmetry mismatch between a preferred hydration shell and the channel structure: we have no idea whether this has energetic consequences. We show these structures and raise this issue because it is interesting. We have a very limited understanding of water and ion interactions with hydrophobic surfaces, especially when the surfaces are concave.

ACKNOWLEDGMENT

We thank the staff at the Cornell High Energy Synchrotron Source A1 and the National Synchrotron Light Source X-25 for help in data collection. We thank A. Kaufman for help with protein purification and crystallization, and Q. Jiang for a critical review of the manuscript.

REFERENCES

1. Parsegian, A. (1969) Energy of an ion crossing a low dielectric membrane: Solutions to four relevant electrostatic problems. *Nature 221*, 844−846.
2. Doyle, D. A., Morais Cabral, J., Pfuetzner, R. A., Kuo, A., Gulbis, J. M., Cohen, S. L., Chait, B. T., and MacKinnon, R. (1998) The structure of the potassium channel: molecular basis of K^+ conduction and selectivity. *Science 280*, 69−77.
3. Zhou, Y., Morais-Cabral, J. H., Kaufman, A., and MacKinnon, R. (2001) Chemistry of ion coordination and hydration revealed by a K^+ channel-Fab complex at 2.0 Å resolution. *Nature 414*, 43−48.
4. Roux, B., and MacKinnon, R. (1999) The cavity and pore helices in the KcsA K^+ channel: electrostatic stabilization of monovalent cations. *Science 285*, 100−102.
5. Zhou, Y., and MacKinnon, R. (2003) The occupancy of ions in the K^+ selectivity filter: charge balance and coupling of ion binding to a protein conformational change underlie high conduction rates. *J. Mol. Biol. 333*, 965−975.
6. Otwinowski, Z., and Minor, W. (1997) Processing of X-ray diffraction data collected in oscillation mode. *Methods Enzymol. 276*, 307−326.
7. Brunger, A. T., Adams, P. D., Clore, G. M., DeLano, W. L., Gros, P., Grosse-Kunstleve, R. W., Jiang, J. S., Kuszewski, J., Nilges, M., and Pannu et al. (1998) Crystallography & NMR system: A new software suite for macromolecular structure determination. *Acta Crystallogr., Sect D: Biol. Crystallogr. 54*, 905−921.
8. Jones, T. A., Zou, J. Y., Cowan, S. W., and Kjeldgaard. (1991) Improved methods for building protein models in electron density maps and the location of errors in these models. *Acta Crystallogr., Sect A: Found. Crystallogr. 47*, 110−119.
9. Morais-Cabral, J. H., Zhou, Y., and MacKinnon, R. (2001) Energetic optimization of ion conduction rate by the K^+ selectivity filter. *Nature 414*, 37−42.
10. Collaborative Computational Project number 4, The CCP4 suite: programs for protein crystallography. (1994) *Acta Crystallogr., Sect. D: Biol. Crystallogr. 50*, 760−763.
11. Kleywegt, G. J., and Jones, T. A. (1996) xdlMAPMAN and xdlDATAMAN−programs for reformatting, analysis and manipulation of biomacromolecular electron-density maps and reflection data sets. *Acta Crystallogr., Sect. D*: *Biol. Crystallogr. 52*, 826−828.
12. Nimigean, C. M., and Miller, C. (2002) Na^+ block and permeation in a K^+ channel of known structure. *J. Gen. Physiol. 120*, 323−335.
13. Neyton, J., and Miller, C. (1988) Discrete Ba^{2+} block as a probe of ion occupancy and pore structure in the high-conductance Ca^{2+}-activated K^+ channel. *J. Gen. Physiol. 92*, 569−586.
14. Jiang, Y., and MacKinnon, R. (2000) The barium site in a potassium channel by X-ray crystallography. *J. Gen. Physiol. 115*, 269−272.
15. Jiang, Y., Lee, A., Chen, J., Cadene, M., Chait, B. T., and MacKinnon, R. (2002) The open pore conformation of potassium channels. *Nature 417*, 523−526.
16. Jiang, Y., Lee, A., Chen, J., Cadene, M., Chait, B. T., and MacKinnon, R. (2002) Crystal structure and mechanism of a calcium-gated potassium channel. *Nature 417*, 515−522.
17. Kraulis, P. J. (1991) MOLSCRIPT: a program to produce both detailed and schematic plots of protein structures. *J. Appl. Crystallogr. 24*, 946−950.
18. Merritt, E. A., and Bacon, D. J. (1997) Raster3D: Photorealistic molecular graphics. *Methods Enzymol. 277*, 505−524.

BI049876Z